World Academy of Science, Engineering and Technology
International Journal of Mechanical and Mechatronics Engineering
Vol:18, No:1, 2024

Improved Simultaneous Performance in the Time Domain and in the Frequency Domain

Azeddine Ghodbane, David Bensoussan, Maher Hammami

***Abstract*—**In this study, we introduce an alternative adaptive architecture that enhances both time and frequency performance, helpfully mitigating the effects of disturbances from the input plant and external disturbances affecting the output. To facilitate superior performance in both the time and frequency domains, we have developed a user-friendly interactive design methods using the GeoGebra platform.

***Keywords*—**Control theory, decentralized control, sensitivity theory, input-output stability theory, robust multivariable feedback control design.

I. Introduction

THE proposed control method can be applied to unstable and invertible plants described by their transfer function. It is based on sensitivity minimization combined with quasi linear control. In a quasi-linear controller, the gain and the poles of the compensator are interrelated [1]. The quasi-linear control method can be illustrated on a Nichols chart: when the gain is increased, the pole is also increased in such a way that the critical point ($0\ dB$, 180°) is avoided. Doing so, stability with an acceptable gain margin is maintained. The advantages of high gain feedback are improved sensitivity and improved tracking.

The design of the quasi linear controller has been formalized for the case of a second order system [2] allowing arbitrarily fast and robust tracking by feedback. The result has been extended to a transfer function of any order [3]. However, implementation of a quasi linear controller has shown that it applies perfectly only when the gain is increased unboundedly.

As a remedy to this problem, the B control method [4], [5] has been proposed. The gain to pole dependency is calibrated differently. It has been shown that for the same gain, B control offers better settling times while keeping the system stable. It has been tested for the control of the arm of a hard disk [6], the orientation of a satellite antenna [7], a levitation system [8] and the control of a drone [9], [10]. Simulations have also shown that integrating a B controller to a L1 adaptive controller results in a better settling time, as well as an improved attenuation of the effects of plant input and plant output perturbations on the feedback system output [11].

Moreover, it has been shown that B control can be extended to multivariable unstable and invertible system and ensures decentralized control [12].

II. Heuristic Presentation of the SISO B Controller

The B compensator structure [1] is represented in Fig. 1.

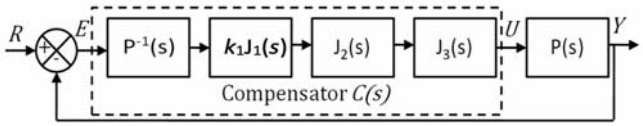

Fig. 1 Structure of the compensator C(s)

Note that the closed loop transmission $T(s)$ and the sensitivity $S(s)$ are related to the output, the input and the error signal as follows:

$$Y(s) = T(s)R(s), \text{ with } T(s) = P(s)C(s)\big(1 + P(s)C(s)\big)^{-1} \quad (1)$$

$$E(s) = S(s)R(s), \text{ with } S(s) = \big(1 + P(s)C(s)\big)^{-1} \quad (2)$$

$$T(s) + S(s) = 1 \quad (3)$$

We will present the case where the plant P(s) is minimum phase, i.e. it is stable and invertible [13] and has the attenuation property, i.e. there exist constants c and q at a frequency high enough such that

$$|P(j\omega)| > \frac{c}{|s|^q}, \text{ for all } |s| > \omega_0 \quad (4)$$

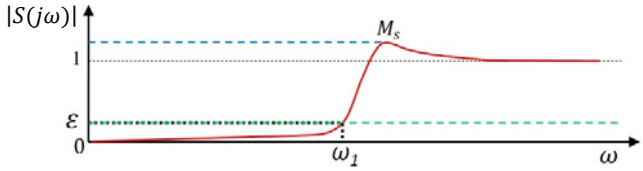

Fig. 2 Modulus of the sensitivity in the SISO case

The design of the series compensator aims at havening sensitivity on a limited frequency range ω_1 smaller than any positive constant ε and the sensitivity norm is less than any constant M_s greater than unity (Fig. 2).

$$\|(1 + PC)^{-1}\|_{\infty} < M_s, M_s > 1 \quad (5)$$

$$\|(1 + PC)^{-1}\|_{\omega_1} < \varepsilon, 0 < \varepsilon < 1 \quad (6)$$

Azeddine Ghodbane and David Bensoussan are with the École de Technologie Supérieure, Montreal, Canada (e-mail: azeddine.ghodbane@etsmtl.ca, david.bensoussan@etsmtl.ca).

Maher Hammami is with University of Sfax, Tunisia (e-mail: hammami_maher@yahoo.fr).

$$C(s) = P^{-1}(s)J_1(s)J_3(s) = P^{-1}(s)\left(\frac{k_1}{s+\omega_1}\right)\left(\frac{\omega_2}{s+\omega_2}\right)^k \quad (7)$$

k, k_1, ω_1 and ω_2 are chosen according to the following criteria. We keep in mind that the addition of phase circuits in the mid frequencies allows to better tune the time response and we assume for now that $J_2(s) = 1$.

$$k \geq n \quad (8)$$

$$k_1 \geq \max\left[2^{(k+1)/2}\omega_1\left(\frac{1+\varepsilon}{\varepsilon}\right), \omega_1\left(\frac{M_s-1}{M_s}\right)\right] \quad (9)$$

$$\omega_b > \omega_1\left[\frac{k_1^2}{\omega_1^2\left(1-\frac{1}{M_S}\right)^2} - 1\right]^{1/2} \quad (10)$$

$$k\tan^{-1}\left(\frac{\omega_b}{\omega_2}\right) + \tan^{-1}\left(\frac{\omega_b}{\omega_1}\right) < \frac{\pi}{2} \quad (11)$$

$$\omega_2 > \max(\omega_b, s_0) \quad (12)$$

III. The Quasi Linear Controller

Given the plant represented by rational functions of the complex variable s with the form $P(s) = \frac{N_P(s)}{D_P(s)}$ and a compensator represented by $C(s) = k\frac{N_C(s)}{D_C(s)}$, the closed loop is represented by:

$$\frac{Y(s)}{R(s)} = T(s) = k\frac{N_P(s)N_C(s)}{1 + kD_P(s)D_C(s)} \quad (13)$$

Let d represent the excess of poles over zeros of $T(s)$ and f be a real number $(d-1)f < 1 < df$.

$Fot\ k > 0$ large the closed loop transfer function is:

$$T_k(s) = T_{zk}(s)T_{dk}(s) \quad (14)$$

$$T_{zk}(s) = \frac{(s+z_1)(s+z_2)\ldots(s+z_m)}{(s+\tilde{z}_1)(s+\tilde{z}_2)\ldots(s+\tilde{z}_m)}, \mathrm{Re}[z_1] \leq \cdots \leq \mathrm{Re}[z_m] \quad (15)$$

$$T_{dk}(s) = \frac{k}{(s+\tilde{p}_1)\ldots(s+\tilde{p}_d)}, \quad Re[\tilde{p}_1] \leq \cdots \leq Re[\tilde{p}_d] \quad (16)$$

It has been shown [2] that when k approaches infinity, the poles $\tilde{z}_1$ are approaching the zeros z_i so that we can concentrate on $T_{dk}(s)$, the poles of which take negative real values, the module of which becomes bigger as the gain increases, ensuring the stability and the fast response of the feedback system.

The compensator takes the form:

$$C_k(s) = \frac{k(s+z_1)(s+z_2)\ldots(s+z_{d-1})}{(s+a_1k^f)(s+a_2k^f)\ldots(s+a_{d-1}k^f)} \quad (17)$$

where the constant a_1 is given by:

$$k^{1-(d-1)f}\tilde{p}_1 = \frac{1}{a_1\ldots a_{d-1}}, \tilde{p}_i = a_ik^f, i > 1 \quad (18)$$

As an example, for $P(s) = \frac{1}{s^2}$, the linear compensator $C(s) = \frac{k(s+1)}{(s+2)}$ is modified to become gain dependent:

$$C_k(s) = \frac{k(s+1)}{(s+2k^{0.6})},\ d = 2, f = 0{,}6 \in \left(\frac{1}{2}, \frac{1}{1}\right) \quad (19)$$

Figs. 3 and 4 show how the stability the stability of the feedback system is maintained after the introduction of a quasi linear controller: as the gain increases, so does the pole $\tilde{p}_1$ so that the Nichols chart keeps a secure distance from the critical point $(0\ dB, 180^\circ)$.

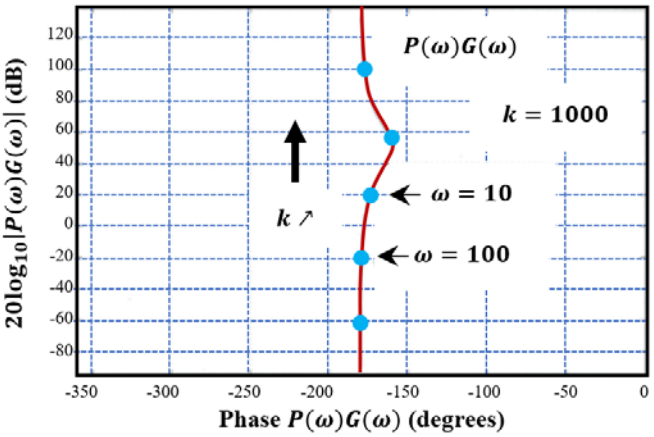

Fig. 3 Nichols chart without using the quasi linear controller [3]

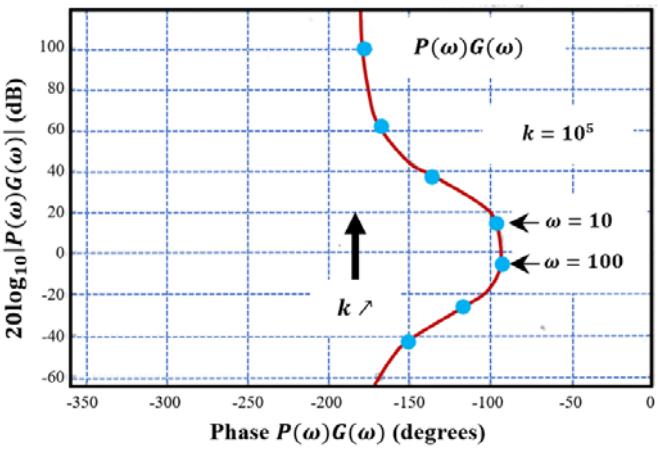

Fig. 4 Nichols chart using the quasi-linear controller [3]

IV. The Stable and Invertible Case

We apply the B control to the design of the controller of a hard disk (Fig. 5).

The arm of a hard disk model is given by [14]:

$$P(s) = \frac{6.4013\times10^7}{s^2}\prod_{i=1}^{4}P_{r,i}(s) \quad (20)$$

with:

$$P_{r,1}(s) = \frac{0.912s^2+457.4s+1.433\times10^8}{s^2+359.2s+1.433\times10^8} \quad (21)$$

$$P_{r,2}(s) = \frac{0.7586s^2+962.2s+2.491\times10^8}{s^2+789.1s+2.491\times10^8} \quad (22)$$

$$P_{r,3}(s) = \frac{9.917\times10^8}{s^2+1575s+9.917\times10^8} \quad (23)$$

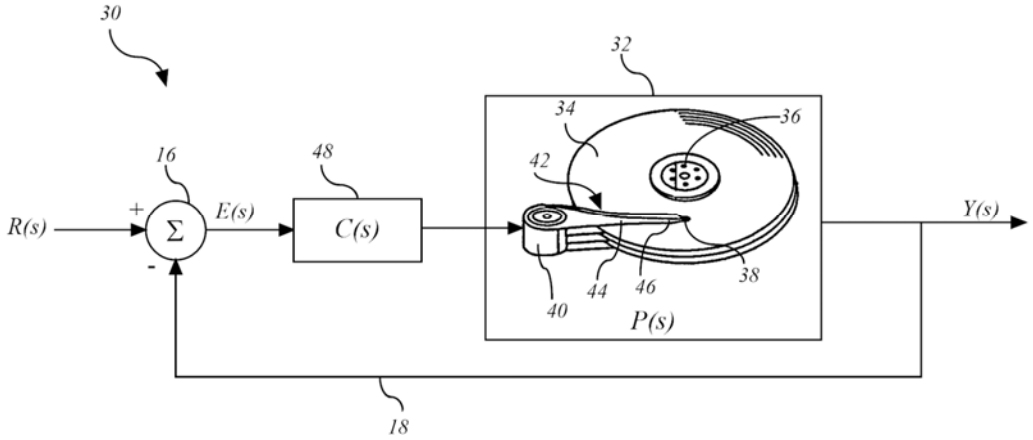

Fig. 5 B controller design of the control of the arm of a hard disk

$$P_{r,4}(s) = \frac{2.731\times10^9}{s^2+2613s+2.731\times10^9} \quad (24)$$

$$C(s) = P^{-1}(s)J(s) \quad (25)$$

$$P(s)C(s) = J(s) = J_1(s)J_2(s)J_3(s) \quad (26)$$

$k_1J_1(s)$ is the transfer function of a high gain filter having an fast time response. For example, $J_1(s)$ can have the following form:

$$J_1(s) = k_1\left(\frac{\omega_1}{s+\omega_1}\right) \quad (27)$$

The $J_2(s)$ compensator contains a set of lead/lag compensator elements operating in the intermediate frequency range. For example, $J_2(s)$ can have the following form:

$$J_2(s) = \prod_{i=1}^{n}\frac{s+z_i}{s+p_i} \quad (28)$$

$J_3(s)$ is the transfer function of a low-pass filter acting at a very high frequency so as to ensure that the controller $C(s)$ remains strictly proper. It can have the general form:

$$J_3(s) = \Pi_{i}^{k}{}_{=1}\frac{\omega_{2i}}{s+\omega_{2i}} \quad , \quad k \geq q \quad (29)$$

Note that the choice of ω_{2i} could be reduced in various ways to improve the implementation, such as a reduction in energy requirements. The compensator parameters [15] are given by $n = 2,\ \omega_1 = 50,\ \omega_B = 13\times10^4,\ p_1 = p_2 = 50,\ z_1 = z_2 = 33, q = k = 6, k_1 = 6223$. $\omega_{2i} = \omega_2$ is a fraction of ω_b.

Our design leads to the following results. Fig. 6 shows the temporal performances when tuning ω_2. It allows the designer to study the effect of the increased bandwidth of the compensator.

Fig. 7 shows the temporal performances when tuning k.

Applying the quasi linear compensator to a hard disk, the settling time is greater than the one that can be obtained with B control for the same compensator gain. However, improvement of the settling time of the quasi linear compensator can be obtained with a much greater and impracticable gain.

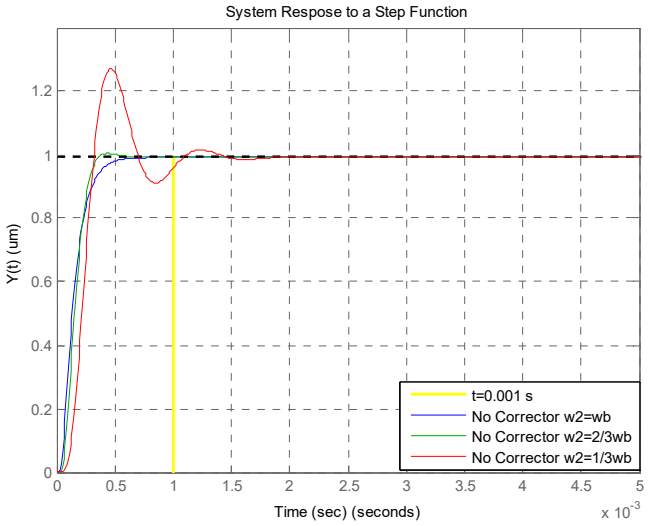

Fig. 6 Temporal response to a step input vs ω_2 [15]

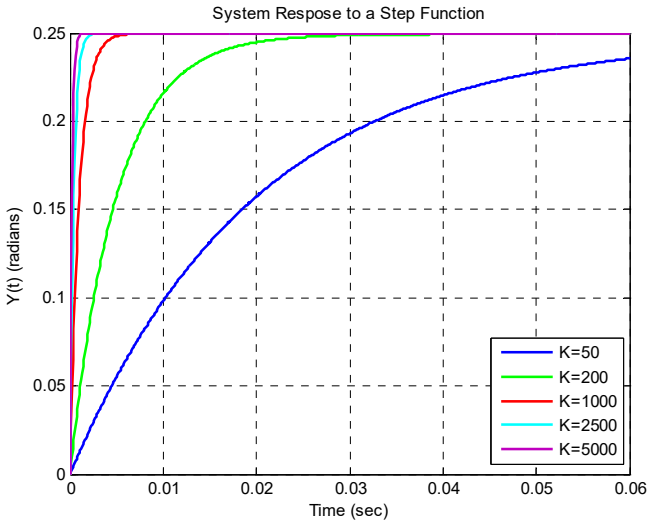

Fig. 7 Temporal response to a step input vs the exponent k [15]

The performances of B controller are compared to existing control methods in Table I. GM and PM represent the Gain

Margin and the Phase margin, t_r and t_s are the rise time and the settling time.

Similarly, the control for positioning satellite antennas is handled. The model of the rigid satellite antenna is presented in Fig. 8 and modelled by the transfer function [7]:

$$P(s) = \frac{1}{s^2+1.72s+1.9} \quad (30)$$

TABLE I
CONTROL OF THE ARM OF THE HARD DISK [6]

Type of control	$GM\ (dB)$	$PM\ (°)$	$t_r\ (s)$	$t_s\ (s)$
Proportional	11.9	12	0.0158	0.406
PID	54.1	47.8	0.0156	0.0637
State feedback	22.8	49	0.0219	0.0738
Quasi Linear	89.8	91.3	4.39	5.95
Present method	13.2	66	0.00019	0.00027

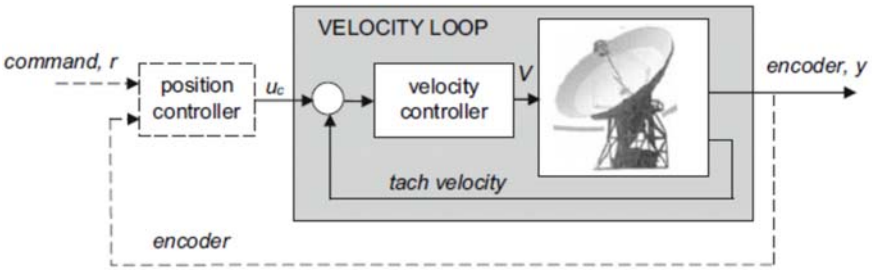

Fig. 8 Closed loop control of the orientation of a satellite [16]

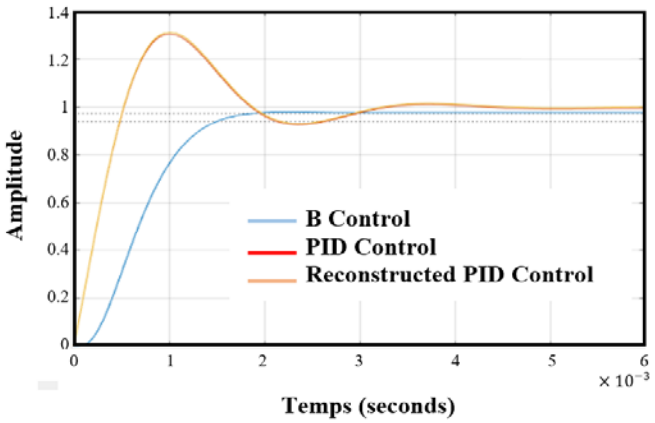

Fig. 9 PID vs B controller for closed loop velocity control [7]

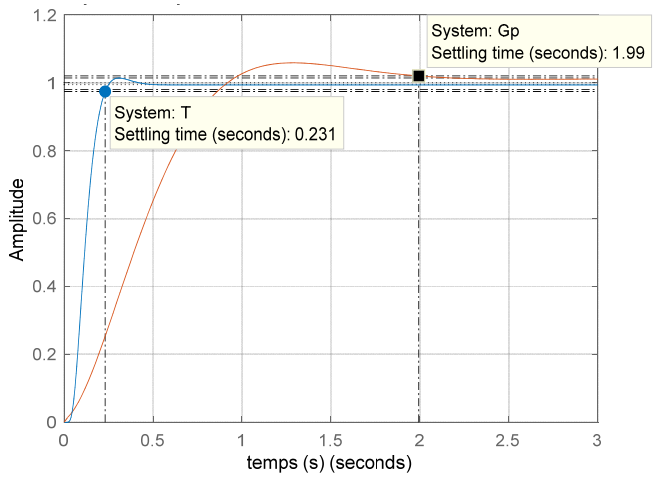

Fig. 10 PID vs B controller for closed loop position control [7]

To compare the B controller to the existing control methods, simulations for the velocity feedback and the position feedback are compared to those obtained by PID controllers and were published in the literature.

The PID is defined as follows [7]:

$$C_{PID}(s) = 99.6827 + 0.03\frac{1}{s+9.8203} - 903.9207.s \quad (31)$$

The parameters of the B controller follow: $\omega_1 = 42$, $\omega_2 = 10750$, $k_1 = 37$, $k = 3$.

Figs. 9 and 10 present the improvements achieved for the step time response for the velocity feedback and the position feedback loops.

Table II presents the time and frequency performances of PID and B controllers.

TABLE II
CONTROL OF A SATELLITE ANTENNA [7]

Type of control	Velocity feedback		Position feedback	
	PID	B	PID	B
$PM\ (°)$	46.7	70.3	147	63
$GM\ (dB)$	∞	14.9	∞	12
$OS\ (\%)$	30	0.06	15.2	0.12
t_s (s)	4	1.5	3.5	0.45

V. THE UNSTABLE AND INVERTIBLE CASE

The unstable process can be decomposed into the product of its minimum-phase part $P_1(s)$ and its unstable part $P_2(s)$, so that the process $P(s)$ is represented by:

$$P(s) = P_1(s)P_2(s) \quad (32)$$

A transfer function $H(s)$ can be defined such that, for some value s_0:

$$H(s) = \left[\frac{c}{(s+s_0)^q}\right] P_2^{-1}(s)P(s) = \frac{c}{(s+s_0)^q} P_1(s) \quad (33)$$

So that $H(s)$ has the same behavior as $P(s)$ at high frequency.

$$\|P(s)H(s)^{-1} - 1\| < \alpha < 1 \quad (34)$$

where α is a value less than unity. Note that $H(s)$ is holomorphic by its design and that its inverse is holomorphically invertible in $Re(s) \geq 0$. The controller $C(s)$ is designed as follows:

$$C(s) = H^{-1}(s)J(s) = \left(\frac{1}{c}\right)(s+s_0)^q P_1^{-1}(s)J(s) \quad (35)$$

So that the loop gain is $P(s)C(s) = P(s)H^{-1}(s)J(s)$. For example, we could choose:

$$J(s) = J_1(s)J_2(s)J_3(s) = \frac{k_1\omega_1}{(s+\omega_1)}\prod_{i=1}^{n}\frac{(s+zi)}{(s+pi)}\left[\frac{\omega_2}{(s+\omega_2)}\right]^k \quad (36)$$

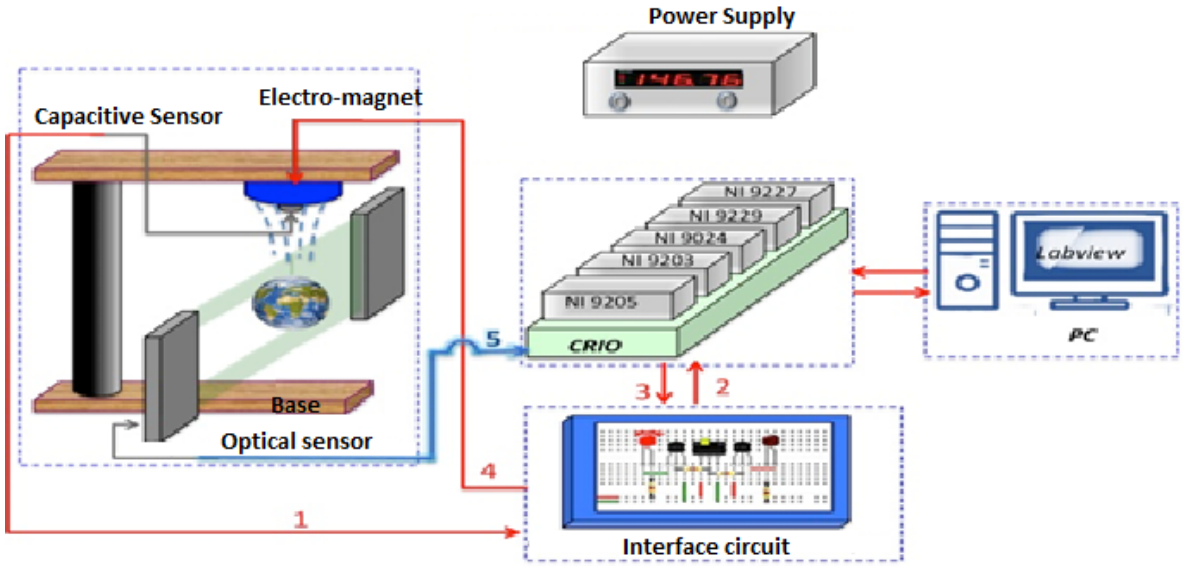

Fig. 11 Magnetic levitation system: Experimental setup

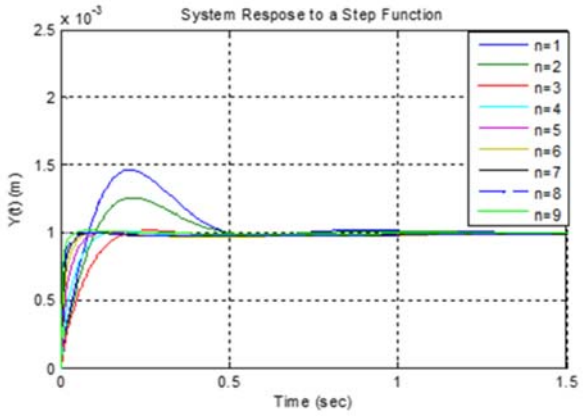

Fig. 12 Time response of B controller for different values of n [8]

We apply the B control design to a levitation system which is open loop unstable (Fig. 11):

$$P(s) = P_1(s)P_2(s) = \frac{-7817.5}{(s-30.51)(s+31.34)(s+184.38)} \quad (37)$$

with:

$$P_1(s) = \frac{-7817.5}{(s+31.34)(s+184.38)} \quad (38)$$

$$P_2(s) = \frac{1}{(s-30.51)} \quad (39)$$

$$P(s)C(s) = P(s)H^{-1}(s)J(s) = \frac{1}{c}(s+s_0)^q J(s)P_2(s) \quad (40)$$

which leads to

$$C(s) = \frac{-\left(5000 + 1000\frac{(n-1)}{2}\right)^2\left(1+\frac{s}{70}\right)\left(1+\frac{s}{3}\right)\left(1+\frac{s}{31.38}\right)\left(1+\frac{s}{184.38}\right)}{\left(1+\frac{s}{100}\right)\left(1+\frac{s}{0.019}\right)\left(1+\frac{s}{3000}\right)} \quad (41)$$

The index n is modified to increase the value of the gain. Fig. 12 shows the time response using B controller.

Applying the proposed compensator with $\omega_2 = 3000\ rad/s$, $k = 3, s_0 = 3$, $\omega_1 = 0.019$, $z_1 = 70$, $p_1 = 100$ and $K_{sc} = -6100$:

$$C(s) = \frac{-6100\left(1+\frac{s}{3}\right)\left(1+\frac{s}{70}\right)\left(1+\frac{s}{31.3407}\right)\left(1+\frac{s}{184.378}\right)}{\left(1+\frac{s}{0.019}\right)\left(1+\frac{s}{100}\right)\left(1+\frac{s}{3000}\right)^3} \quad (42)$$

The simulation results using (42) lead to the following optimal values [8], [17]: Static gain of the compensator $K_{sc} = 6100$, $t_r = 60ms$, $t_s = 60ms$, overshoot: $D\,\% = 1.25\%$, $GM = 4.92\ dB$, and $PM = 68.6^{\circ}$.

For a sampling time of 10 ms, the digital compensator $C(z)$ is:

$$C(z) = \frac{n_4z^4+n_3z^3+n_2z^2+n_1z+n_0}{z^5+d_4z^4+d_3z^3+d_2z^2+d_1z+d_0} \quad (43)$$

$$C(z) = \frac{-37.9z^4+46.54z^3-9.372z^2-1.159\times10^{-6}z-1.25\times10^{-19}}{z^5-1.368z^4+0.368z^3-1.033\times10^{-13}z^2+9.611\times10^{-27}z-3.09\times10^{-40}} \quad (44)$$

The performances of time response using the B controller are compared to the PID controller. These controllers have been applied to the same experimental setup. Figs. 13 and 14 illustrate this comparison.

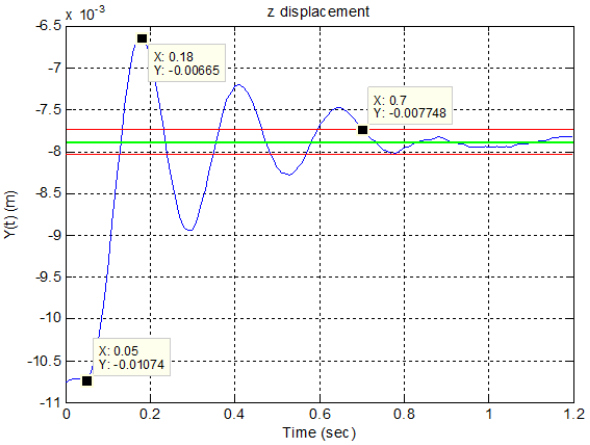

Fig. 13 PID control of a levitation system [17]

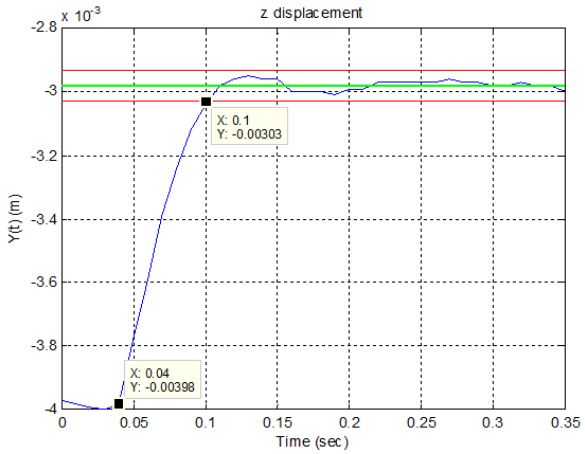

Fig. 14 B control of a levitation system [17]

Fig. 15 shows the effects of the various Nyquist diagrams plotted with GeoGebra software for:

$$J_2(s) = \frac{\left(1+\frac{s}{z_1}\right)\left(1+\frac{s}{z_2}\right)}{\left(1+\frac{s}{p_1}\right)\left(1+\frac{s}{p_2}\right)} \tag{45}$$

with: $z_1 = 3.7, p_1 = 3.9, z_2 = 8.5, p_2 = 10.8$

Similarly, B control has been successfully applied to the control of a drone [9], [10].

VI. The L1 Adaptive Control Case

The insertion of the low pass filter $C(s)$ decouples the high frequency adaptation feedback from the feedback system loop. $C(s)$ is usually a simple pole low pass filter. In Fig. 15, z is the output of the plant that takes into consideration the effects of input and output plant perturbation n and σ. The plant input v takes in consideration the plant input perturbation σ. The adaptation feedback gain (the MIT gain) $\hat{\sigma} = \frac{\gamma}{s}$ amplifies the error signal $\tilde{x} = z - \hat{x}$. The input of the feedback system r is multiplied by a constant gain k_r.

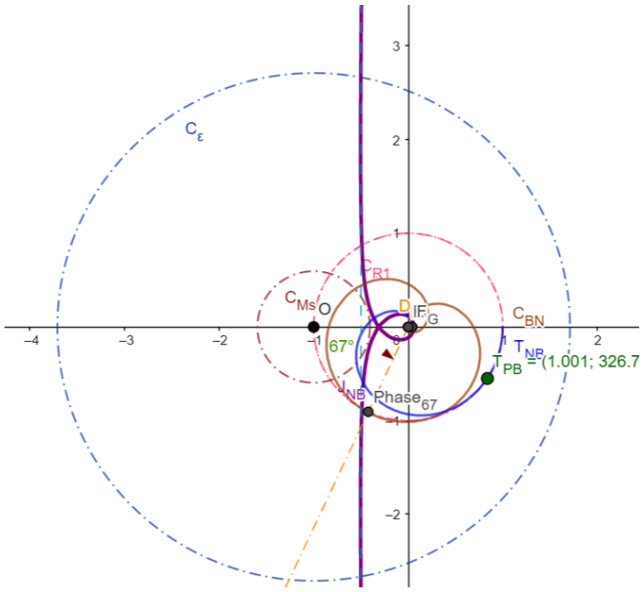

Fig. 15 Nyquist diagram of $J(s)$ [4]

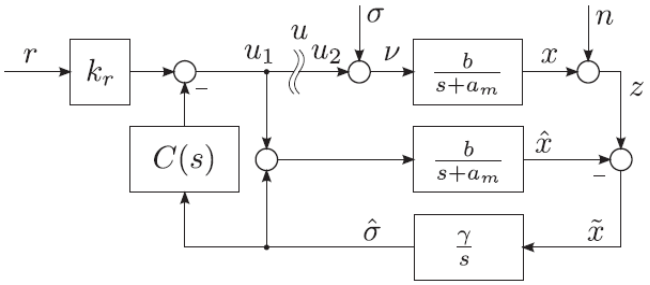

Fig. 16 Architecture L1 [18]

Application of Masson formula (Fig. 16) leads to the following relations:

$$\begin{bmatrix} x \\ z \\ u \\ v \end{bmatrix} = \begin{bmatrix} H_{zr}(s) & H_{z\sigma}(s) & H_{zn}(s)-1 \\ H_{zr}(s) & H_{z\sigma}(s) & H_{zn}(s) \\ P^{-1}(s)H_{zr}(s) & P^{-1}(s)H_{z\sigma}(s)-1 & P^{-1}(s)\left(H_{zn}(s)-1\right) \\ P^{-1}(s)H_{zr}(s) & P^{-1}(s)H_{z\sigma}(s) & P^{-1}(s)\left(H_{zn}(s)-1\right) \end{bmatrix} \begin{bmatrix} r \\ \sigma \\ n \end{bmatrix} \tag{46}$$

with:

$$\mathrm{H_{xr}(s)} = \frac{\mathrm{k_r(1+P_m(s)\Gamma(s))P(s)}}{\mathrm{1+P_m(s)\Gamma(s)+C(s)\Gamma(s)(P(s)-P_m(s))}} \tag{47}$$

$$H_{x\sigma}(s) = \frac{(1+\Gamma(s)P_m(s)-C(s)\Gamma(s)P_m(s))P(s)}{1+P_m(s)\Gamma(s)+C(s)\Gamma(s)(P(s)-P_m(s))} \tag{48}$$

$$H_{xn}(s) = \frac{-C(s)\Gamma(s)P(s)}{1+P_m(s)\Gamma(s)+C(s)\Gamma(s)(P(s)-P_m(s))} \tag{49}$$

For the particular case: $P(s) = P_m(s) = \frac{b}{s+a_m}$, $\Gamma(s) = \frac{\gamma}{s}$ and $P_1(s) = s^2 + a_m s + b\gamma$, we get:

$$\begin{bmatrix} x \\ z \\ u \\ v \end{bmatrix} = \begin{bmatrix} \frac{k_r b}{s+a_m} & \left(1-\frac{b\gamma C(s)}{P_1(s)}\right)P_m(s) & -\frac{b\gamma C(s)}{P_1(s)} \\ \frac{k_r b}{s+a_m} & \left(1-\frac{b\gamma C(s)}{P_1(s)}\right)P_m(s) & 1-\frac{b\gamma C(s)}{P_1(s)} \\ k_r & \frac{-b\gamma C(s)}{P_1(s)} & -\frac{\gamma C(s)(s+a_m)}{P_1(s)} \\ k_r & 1-\frac{b\gamma C(s)}{P_1(s)} & -\frac{\gamma C(s)(s+a_m)}{P_1(s)} \end{bmatrix} \begin{bmatrix} r \\ \sigma \\ n \end{bmatrix} \quad (50)$$

It is wise to study the stability of the loop $L_{u_1u_2}$ (Fig. 16).

$$L_{u_1u_2} = \frac{u_1}{u_2} = -\frac{C(s)(1+\Gamma(s)P_m(s))^{-1}\Gamma(s)P(s)}{1-C(s)(1+\Gamma(s)P_m(s))^{-1}\Gamma(s)P_m(s)} \quad (51)$$

which leads to:

$$L_{u_1u_2} = -\frac{\gamma bC(s)}{s(s+a_m)+b\gamma(1-C(s))} = -\frac{\gamma bC(s)}{P_1(s)-\gamma bC(s)} \quad (52)$$

One example of integration of B control and L1 adaptive control is the BL1 architecture (Fig. 17).

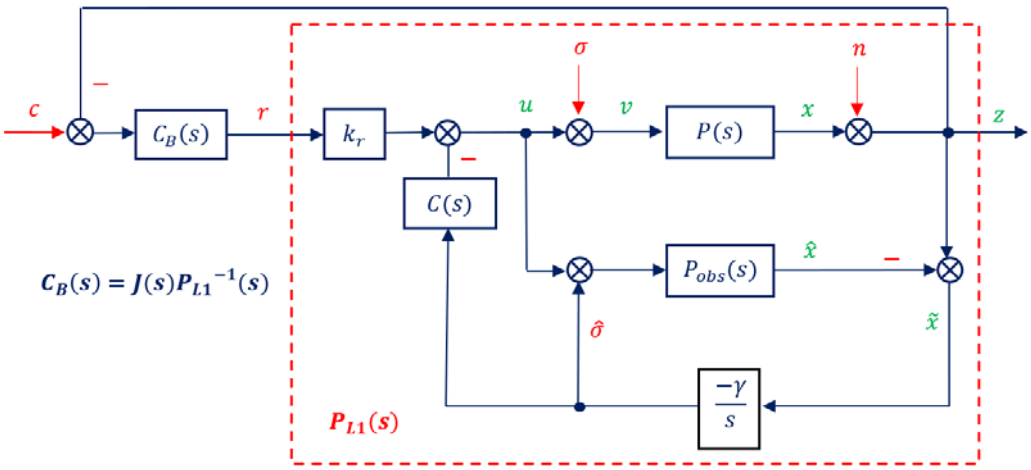

Fig. 17 BL1 architecture [11]

$C_B(s)$ is a serial B controller applied to the L1 adaptive system of Fig. 17. This scheme leads to the following relations:

$$H_{zc}(s) = \frac{P(s)C_B(s)}{1+P(s)C_B(s)+C(s)\Gamma(s)(1+\Gamma(s)P_m(s))^{-1}(P(s)-P_m(s))} \quad (53)$$

$$H_{z\sigma}(s) = \frac{1-C(s)(1+\Gamma(s)P_m(s))^{-1}\Gamma(s)P_m(s)}{1+P(s)C_B(s)+C(s)\Gamma(s)(1+\Gamma(s)P_m(s))^{-1}(P(s)-P_m(s))}P(s) \quad (54)$$

$$H_{zn}(s) = \frac{1-C(s)(1+\Gamma(s)P_m(s))^{-1}\Gamma(s)P_m(s)}{1+P(s)C_B(s)+C(s)\Gamma(s)(1+\Gamma(s)P_m(s))^{-1}(P(s)-P_m(s))} \quad (55)$$

The gang of six of the system described in Fig. 17 is:

$$\begin{bmatrix} x \\ z \\ u \\ v \end{bmatrix} = \begin{bmatrix} H_{zc}(s) & H_{z\sigma}(s) & H_{zn}(s)-1 \\ H_{zc}(s) & H_{z\sigma}(s) & H_{zn}(s) \\ P^{-1}(s)H_{zc}(s) & P^{-1}(s)H_{z\sigma}(s)-1 & P^{-1}(s)\left(H_{zn}(s)-1\right) \\ P^{-1}(s)H_{zc}(s) & P^{-1}(s)H_{z\sigma}(s) & P^{-1}(s)\left(H_{zn}(s)-1\right) \end{bmatrix} \begin{bmatrix} c \\ \sigma \\ n \end{bmatrix} \quad (56)$$

For the particular case: $P(s) = P_m(s) = \frac{b}{s+a_m}$, $\Gamma(s) = \frac{\gamma}{s}$ and $P_1(s) = s^2 + a_m s + b\gamma$, the new open loop gain is given by:

$$J(s) = H_{xr}(s)C_B(s) = \frac{k_r(1+P_m(s)\Gamma(s))P(s)}{1+P_m(s)\Gamma(s)+C(s)\Gamma(s)(P(s)-P_m(s))} = k_r P(s)C_B(s) \quad (57)$$

Simulation of the plant output versus the feedback system input c, the plant perturbation input σ and the plant output n respectively applied at times 0, 1 and 10 seconds. Fig. 18 shows the time response improvement of BL1 architecture over the L1 architecture.

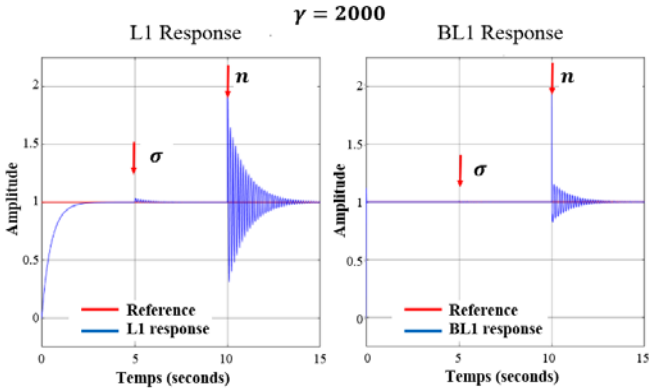

Fig. 18 The effect of plant perturbations - L1 vs BL1 [11]

VII. Conclusion

B control exhibits tangible advantages for the minimum phase case such as the control of a hard disk or a satellite antenna, for the unstable and invertible SISO case exemplified by the levitation experiment, as well as the MIMO unstable (but invertible) case [12]. It can also improve the L1 adaptive control. Time response improvements were obtained while maintaining appreciable gain and phase margins.

Research on the B control method can be extended to time delay systems, internal model control, state space formulations and nonlinear systems.

REFERENCES

[1] Bensoussan, David. System and method for feedback control, P, US Patent 8,831,755, Deposited September 9, 2014.
[2] Kelemen, Mattei, 2002, Arbitrarily fast and robust tracking by feedback, International Journal of Control, 75, 443-465
[3] Kelemen, Bensoussan David, "On the Design, Robustness, Implementation and Use of Quasi-Linear Feedback Compensator", International Journal of Control, 15 avril 2004, Vol 77, No 6, pp 527-545 - 77, no. 6 (2004): 527-545
[4] Bensoussan David, Benkhellat Lyes, Geogebra as a tool of design of ultrafast and robust controller, 2017 IEEE International Conference on Industrial Technology, Toronto, March 22-25, 2017.
[5] Bensoussan David, Robust and Ultrafast Response Compensator for Unstable Invertible Plants, Automatica, Volume 60, Octobre 2015 pp. 43-47, 2015.
[6] Bensoussan David, Sun Yulan, Hammami Maher, "Robust and ultrafast design of a control system based on optimal sensitivity and optimal complementary sensitivity", The 14th international conference on Sciences and Techniques of Automatic control & computer engineering, December 20-22, 2013, Sousse, Tunisia.
[7] Bensoussan David, Houimdi Amine, Hammami Maher, Sun Yulan, Loo Darren, Brossard Jeremy, Demonstration of a New Control Method for Positionning Satellite Antennas, Internal Report INNOV B, École de technologie supérieure, 2020.
[8] Sun. Yulan, Bensoussan David, Hammami M, Wang Tao., and Houimdi Amine, Robust and Ultrafast Response Compensator Applied to a Levitation System, European Control Conference ECC15, Linz, Austria, July 15-17, 2015.
[9] Brossard Jeremy, Bensoussan David, Landry René, Hammami Maher, A new fast compensator design applied to a quadcopter, 2019 8th International Conference on Systems and Control, Octobre 2019, Marrakech, Maroc.
[10] Brossard Jeremy, Bensoussan David, Landry René, Hammami Maher, Robustness Studies on Quadrotor Control, International Conference on Unmanned Aircraft Systems, ICUAS'19, Atlanta, GA, USA, on June 11-14 2019.
[11] Ghodbane Azeddine, Madali Adem Soufiane, Bensoussan David, and Hammami Maher An improved L1 Adaptive controller, 2022 10th International Conference on Systems and Control (ICSC), 23-25 novembre 2022.
[12] Bensoussan David, Brossard Jérémy, Decentalized and ultrafast control, 21st International Conference on System Theory, Control and Computing, Sinaia, Romania, October 19 – 21, 2017.
[13] Bensoussan, D. Sensitivity reduction in single-input single-output systems, International Journal of Control, Vol. 39, p. 321-335, 1984. https://doi.org/10.1080/00207178408933168
[14] Chen Ben M., Lee T. H., Peng K., Venkataramanan V., Hard Disk Drive Servo Systems, Springer, 2006.
[15] M. Hammami, D. Bensoussan and Y. Sun, "Fine tuning the time response of a robust and ultrafast compensator," *22nd Mediterranean Conference on Control and Automation*, Palermo, Italy, 2014, pp. 1400-1405, doi: 10.1109/MED.2014.6961572.
[16] Wodek Gawronski. "Modeling and Control of Antenna and Telescopes", Springer Science, 2008.
[17] M.-A. Houimdi, « Ajustement d'un nouvel algorithme d'optimisation simultanée des réponses temporelles et fréquentielles », École de technologie supérieure, MSc. Thesis, 2015.
[18] Kharisov, Evgeny et al. "Comparison of architectures and robustness of model reference adaptive controllers and L1 adaptive controllers." *International Journal of Adaptive Control and Signal Processing* 28 (2014): 633 - 663.